Available online at www.sciencedirect.com
ScienceDirect
Automatica 42 (2006) 1637–1650
automatica
www.elsevier.com/locate/automatica

A speed-sensorless indirect field-oriented control for induction motors based on high gain speed estimation☆

Marcello Montanari[a], Sergei Peresada[b], Andrea Tilli[a,*]

[a]*Department of Electronics, Computer Science and Systems (DEIS), CASY - Center for Research on Complex Automated Systems "G. Evangelisti", Engineering Faculty, University of Bologna, Viale Pepoli 3/2, 40123 Bologna, Italy*
[b]*Department of Electrical Engineering, National Technical University of Ukraine "Kiev Polytechnic Institute", Prospect Pobedy 37, Kiev 252056, Ukraine*

Received 23 June 2005; received in revised form 4 April 2006; accepted 8 May 2006
Available online 28 July 2006

Abstract

The authors design a new speed sensorless output feedback control for the full-order model of induction motors with unknown constant load torque, which guarantees local asymptotic tracking of smooth speed and rotor flux modulus reference signals and local asymptotic field orientation, on the basis of stator current measurements only. The proposed nonlinear controller exploits the concept of indirect field orientation (no flux estimation is required) in combination with a new high-gain speed estimator based on the torque current tracking error. The estimates of unknown load torque and time-varying rotor speed converge to the corresponding true values under a persistency of excitation condition with a physically meaningful interpretation, basically equivalent to non-null synchronous frequency. Stability analysis of the overall dynamics has been performed exploiting the singular perturbation method. The proposed control algorithm is a "true" industrial sensorless solution since no simplifying assumptions (flux and load torque measurements) are required. Simulation and experimental tests show that the proposed controller is suitable for medium and high performance applications.
© 2006 Elsevier Ltd. All rights reserved.

Keywords: Induction motors; Indirect field-oriented control; Lyapunov stability; Speed control

1. Introduction

Vector controlled induction motor (IM) drives are wide spread electromechanical conversion systems for high-dynamic performance applications, where motion control or high precision speed control is needed (Leonhard, 2001). Usually, a digital shaft speed-position sensor is required in these applications. For low dynamic applications such as pumps and fans the typical solution is the so-called "adjustable-speed" drive. This is a simple low-cost voltage–source inverter fed IM drive with scalar voltage frequency control. Voltage frequency controlled drives typically are speed-sensorless, i.e. without the speed-position sensor, according to common nomenclature in electric drive field. An intermediate class of ac drive applications such as elevators and auxiliary machines of rolling mills requires enhanced dynamic performances and wider speed range as compared with "adjustable-speed" drives, but approximatively at the same cost. Typically, for such applications the speed reference ranges are from 1% to 100% of the IM nominal speed (or even more if the field-weakening technique is adopted, Leonhard, 2001) while the load torque could be up to 100–150% of the rated value. Installation of an encoder for such applications leads to increased cost, reduces reliability, especially in hostile environments, and increases sensitivity to electromagnetic noise. All leading electrical drive producers have already presented in the market sensorless products even if a theoretical framework for IM sensorless control is not well established yet. These reasons stimulated strong research activity in the development of sensorless IM drives in both practically and theoretically oriented motor control research groups.

☆ This paper was not presented at any IFAC meeting. This paper was recommended for publication in revised form by Associate Editor Yong-Yan Cao under the direction of the Editor Mituhiko Araki.
* Corresponding author. Tel.: +39 051 2093924; fax: +39 051 2093073.
E-mail addresses: mmontanari@deis.unibo.it (M. Montanari), peresada@i.com.ua (S. Peresada), atilli@deis.unibo.it (A. Tilli).

0005-1098/$ - see front matter © 2006 Elsevier Ltd. All rights reserved.
doi:10.1016/j.automatica.2006.05.021

There is a large number of investigations related to this problem. Extensive overviews of ac sensorless control strategies are given in Rajashekara, Kawamura, and Matsuse (1996), Vas (1998), and Holtz (2002). According to these references, contributions are concentrated in three main directions: IM spatial saliency methods with fundamental excitation and high-frequency signal injection, extended Kalman filter technique and adaptive system approaches.

Interest in medium and potentially high-performance applications of IM pointed main research efforts in the third direction. In Kubota and Matsuse (1994) a rotor flux observer and a speed estimator are presented, considering the speed as a constant parameter of the IM model. Simplified stability proof is used to construct the parameters estimation algorithms. A rotor flux-speed observer, which is adaptive with respect to rotor resistance, presented in Montanari, Peresada, Tilli, and Tonielli (2000), is based on rigorous Lyapunov stability analysis. Simulation and experimental tests demonstrate the feasibility of the controllers constructed using these flux-speed observation schemes. The hyperstability approach is utilized in Schauder (1992) under the assumption that the rotor flux vector can be detected by integrating the stator current dynamic equation. In order to avoid open loop integration, in Peng and Fukao (1994) the speed-dependent back-EMF vector is computed differentiating the stator currents. A modification of that control algorithm is then proposed considering the instantaneous IM reactive power as an output variable. This solution is stator resistance invariant. Both speed estimation algorithms are constructed considering the rotor speed as a constant parameter. VSS technique for speed estimation is exploited in Doki, Sangwongwanick, and Okuma (1992) and Yan, Jin, and Utkin (2000). In Chern, Chang, and Tsai (1998) the speed estimator, which is adaptive with respect to stator and rotor resistance, is developed using integral variable structure approach and neglecting speed dynamics. Important investigations on the observability properties of sensorless controlled induction motors are reported in Canudas De Wit, Youssef, Barbot, Martin, and Malrait (2000) and Ibarra-Rojas, Moreno, and Espinosa-Perez (2004), where it is shown that the speed and flux state variables are not detectable from current measurements under dc-excitation.

Although an extensive research activity has been carried out during the last decades, from the theoretical viewpoint the IM sensorless control still represents an open research topic due to: (1) strong simplifying assumptions on IM speed dynamics, e.g. motor speed is considered as a constant parameter; (2) pure integration or derivative of the stator currents are needed;(3) only few contributions are based on rigorous closed-loop stability analysis. In Feemster, Aquino, Dawson, and Behal (2001) a semiglobal exponential speed-flux tracking control is developed assuming known load torque and rotor flux measurements (or obtained using open loop integration of the stator voltage equations with zero initial conditions). Under the same simplifying assumptions a globally asymptotically stable (locally exponentially stable) speed-flux tracking control algorithm is proposed in Marino, Tomei, and Verrelli (2002b,2004a). A version of this controller, which is adaptive with respect to rotor resistance variation, is designed in Marino, Tomei, and Verrelli (2002a). Such simplifying assumptions allow to consider the rotor speed as an unknown variable but with known time derivative. Direct application of adaptive estimation using Lyapunov theory is possible for such structure. In Montanari, Peresada, and Tilli (2003) a local exponential speed tracking-flux regulation control algorithm is designed under standard assumption that load torque is unknown but constant. In Marino, Tomei, and Verrelli (2004b) a sensorless controller based on a speed/flux observer is designed, under assumptions of unknown rotor/stator fluxes but with known and smooth load torque. It guarantees local exponential rotor flux tracking with explicitly computable domain of attraction. Under the same hypothesis, a speed-flux tracking controller in Montanari, Peresada, and Tilli (2004) guarantees similar features, provided that persistency of excitation related to IM observability properties is ensured. Nevertheless, all these contributions cannot be considered "true" sensorless solutions since rotor flux information and/or knowledge of load torque are needed for controller implementation.

The aim of this paper is to develop a new true speed-sensorless control for IM speed and flux tracking. For this purpose a new high-gain speed estimator is designed on the basis of the torque current regulation error. The controller development, which is based on the concept of improved indirect-field orientation (Peresada & Tonielli, 2000) leads to feedback interconnected electromechanical (speed) and electromagnetic (flux) subsystems (Peresada, Montanari, Tilli, & Kovbasa, 2002). The fourth order electromechanical dynamics, which is linear if flux regulation errors are zero, is decomposed into the second order mechanical dynamics and the second order torque current regulation and speed estimation subsystems. Applying time-scale separation concept with the speed estimation subsystem designed to be much faster than the mechanical dynamics, a reduced order model for the controlled IM is obtained using singular perturbation technique. The reduced order model is composed of the feedback interconnected linear asymptotically stable mechanical subsystem and the nonlinear electromagnetic subsystem. Finally, it is shown that local asymptotic speed and rotor flux modulus tracking together with asymptotic field orientation are achieved in presence of unknown constant load torque, if persistency of excitation conditions are satisfied and the speed estimation subsystem is designed sufficiently faster than the mechanical dynamics. Stability proof is performed exploiting nonlinear approach based on Lyapunov-like technique, which represents the natural framework for nonlinear IM control and leads to a better understanding of the system properties with respect to other methods, e.g. techniques based on linearization. The proposed nonlinear output feedback controller represents a true sensorless solution, since it has the following features: (A) the full-order IM model is considered; (B) no flux measurement or estimation, based on open-loop integration, is required; (C) it is based only on stator current measurements, without any differentiation; (D) load torque is assumed constant, but unknown; (E) by replacing the speed estimation with the speed measurement, global exponential stability is achieved

(see Peresada & Tonielli, 2000); (F) control objectives of each control subsystems are clearly understandable and a regular tuning procedure for the controller gains can be adopted.

Experimental and simulation tests demonstrate that the achievable performances are close to those which are typically obtained from standard vector control with speed measurements.

The paper is organized as follows. The IM model and control problem statement are given in Section 2. The speed-flux controller and error dynamics are presented and discussed in Section 3. Stability analysis is given in Section 4. Results of experimental and simulation tests are reported in Section 5. Conclusions are given in Section 6.

2. Induction motor model and control problem statement

2.1. Induction motor model

The equivalent two-phase model of the symmetrical IM, under assumptions of linear magnetic circuits and balanced operating conditions, is presented in an arbitrary rotating reference frame (d–q) (Leonhard, 2001) as

$$\begin{aligned}
\dot{\omega} &= \mu(\psi_d i_q - \psi_q i_d) - \frac{T_L}{\mathscr{J}},\\
\dot{i}_d &= -\gamma i_d + \omega_0 i_q + \alpha\beta\psi_d + \beta\omega\psi_q + \frac{1}{\sigma}u_d,\\
\dot{i}_q &= -\gamma i_q - \omega_0 i_d + \alpha\beta\psi_q - \beta\omega\psi_d + \frac{1}{\sigma}u_q,\\
\dot{\psi}_d &= -\alpha\psi_d + (\omega_0 - \omega)\psi_q + \alpha L_m i_d,\\
\dot{\psi}_q &= -\alpha\psi_q - (\omega_0 - \omega)\psi_d + \alpha L_m i_q,
\end{aligned} \tag{1}$$

where $\mathbf{i} = (i_d, i_q)^T$, $\mathbf{\Psi} = (\psi_d, \psi_q)^T$, $\mathbf{u} = (u_d, u_q)^T$ denote stator current, rotor flux and stator voltage vectors. Subscripts d and q stand for vector components in the (d–q) reference frame, ω is the rotor speed, T_L is the load torque and ε_0, $\omega_0 = \dot{\varepsilon}_0$ are the angular position and speed of the (d–q) reference frame with respect to a fixed stator reference frame (a–b), where the physical variables are defined. Transformed variables in (1) are given by

$$\begin{matrix}\mathbf{x}_{dq} = e^{-\mathbf{J}\varepsilon_0}\mathbf{x}_{ab}\\ \mathbf{x}_{ab} = e^{\mathbf{J}\varepsilon_0}\mathbf{x}_{dq}\end{matrix} \quad \text{where } e^{-\mathbf{J}\varepsilon_0} = \begin{bmatrix}\cos\varepsilon_0 & \sin\varepsilon_0\\ -\sin\varepsilon_0 & \cos\varepsilon_0\end{bmatrix}, \tag{2}$$

where $\mathbf{x}_{yz}$ stands for any two-dimensional vector of IM.

Positive constants related to the electrical and mechanical parameters of the IM are defined as $\sigma = L_s(1 - L_m^2/L_s L_r)$, $\beta = L_m/\sigma L_r$, $\mu = \frac{3}{2}L_m/\mathscr{J}L_r$, $\alpha = R_r/L_r$, $\gamma = R_s/\sigma + \alpha L_m\beta$, where $\mathscr{J}$ is the total rotor inertia, R_s, R_r, L_s, L_r are stator/rotor resistances and inductances, respectively, L_m is the magnetizing inductance. One pole pair is assumed without loss of generality. No mechanical friction is supposed.

General specification for speed-controlled electric drives requires to control the two IM outputs, speed and rotor flux modulus, defined as $\mathbf{y}_1 = [\omega, (\psi_d^2 + \psi_q^2)^{1/2}]^T \triangleq (\omega, |\psi|)^T$, using the two-dimensional stator voltage vector $\mathbf{u}$ on the basis of measured variables vector $\mathbf{y}_2 = (i_d, i_q)^T$.

2.2. Control objectives

Define $\mathbf{y}_1^* = (\omega^*, \psi^*)^T$, where ω^* and $\psi^* > 0$ are speed and flux reference trajectories. Speed and flux modulus tracking errors are $\tilde{\omega} = \omega - \omega^*$, $\tilde{\psi} = |\psi| - \psi^*$. Following the concept of indirect field orientation (IFO) (Peresada & Tonielli, 2000) the d- and q-axis flux tracking errors are defined as $\tilde{\psi}_d = \psi_d - \psi^*$, $\tilde{\psi}_q = \psi_q$. Note that $\lim_{t\to\infty}\tilde{\psi}_q = 0$ is the condition of asymptotic field orientation and that the condition $\lim_{t\to\infty}(\tilde{\psi}_d, \tilde{\psi}_q) = 0$ implies $\lim_{t\to\infty}\tilde{\psi} = 0$.

The speed-flux tracking problem is formulated as follows. Consider the IM model (1), (2) and assume that:

(A.1) Stator currents are available for measurement.
(A.2) Motor parameters are exactly known and constant.
(A.3) Load torque T_L is unknown, bounded and constant.
(A.4) Speed and flux reference trajectories ω^*, ψ^* are smooth functions with known and bounded first and second time derivatives; flux reference trajectory is strictly positive, i.e. $\psi^*(t) > 0\ \forall t$.

Under these assumptions, it is required to design an output feedback controller which guarantees local asymptotic speed and rotor flux tracking and asymptotic field orientation, i.e.

$$\lim_{t\to\infty}\tilde{\omega} = 0, \quad \lim_{t\to\infty}\tilde{\psi}_d = 0, \quad \lim_{t\to\infty}\tilde{\psi}_q = 0 \tag{3}$$

with all signals bounded.

3. Speed-flux sensorless control algorithm

The general structure and the basic design approach adopted for the proposed speed-flux sensorless controller are the following. The controller is composed of a feed-forward and a feedback part. The feed-forward part is derived from model inversion assuming smooth references. The feedback one is designed exploiting classical cascade structure for inner current and outer speed-flux control loops. Lyapunov design is applied following the conceptual line reported in Peresada and Tonielli (2000) and introducing a novel speed estimator. The flux controller is based on the improved indirect field-oriented control approach, hence no flux estimation is required. With suitable gain selection, the torque-current tracking and the speed estimation dynamics are imposed much faster than the speed-flux control loops, thus achieving two-time scale property. This feature is crucial for the stability of the overall tracking and estimation error dynamics.

The proposed speed-flux controller and speed estimator are defined as follows:

flux controller:

$$i_d^* = \frac{1}{\alpha L_m}(\alpha\psi^* + \dot{\psi}^*), \tag{4}$$

$$\dot{\varepsilon}_0 = \omega_0 = \hat{\omega} + \alpha L_{\mathrm{m}} \frac{i_q}{\psi^*} + \frac{v_q}{\psi^*},$$
$$v_q = \frac{1}{\beta}\left[\hat{\omega}(1+\gamma_1) + \alpha L_{\mathrm{m}} \frac{i_q}{\psi^*}\right] \tilde{i}_d, \tag{5}$$

$$\gamma_1 = \frac{1}{\alpha}\left(\frac{R_{\mathrm{s}}}{\sigma} + k_{id1}\right); \tag{6}$$

speed controller:

$$i_q^* = \frac{1}{\mu\psi^*}(\dot{\omega}^* + \hat{T}_{\mathrm{L}} - k_\omega e_\omega),$$
$$\dot{\hat{T}}_{\mathrm{L}} = -k_{\omega i} e_\omega; \tag{7}$$

current controller:

$$u_d = \sigma(\gamma i_d^* - \omega_0 i_q - \alpha\beta\psi^* + \dot{i}_d^* - k_{id1}\tilde{i}_d),$$
$$u_q = \sigma(\gamma i_q^* + \omega_0 i_d + \beta\hat{\omega}\psi^* + \dot{i}_q^* - k_{iq1}\tilde{i}_q); \tag{8}$$

speed estimator:

$$\dot{\hat{\omega}} = \dot{\omega}^* - k_{io}\tilde{i}_q; \tag{9}$$

where $\hat{\omega}$ is the speed estimation, $\hat{T}_{\mathrm{L}}$ is the estimation of load constant $T_{\mathrm{L}}/\mathscr{J}$, $e_\omega = \hat{\omega} - \omega^*$ is the estimated speed tracking error, $\tilde{i}_d = i_d - i_d^*$, $\tilde{i}_q = i_q - i_q^*$ are the current tracking errors with respect to references generated by flux and speed controllers. Control tuning parameters in (4)–(9) are the speed controller proportional and integral gains $(k_\omega, k_{\omega i})^{\mathrm{T}} > 0$, the current controllers proportional gains k_{id1}, k_{iq1}, the tuning gain γ_1 and the speed estimator gain $k_{io} > 0$. Additional definitions of estimation errors for speed and torque are $\tilde{\tilde{\omega}} = \omega - \hat{\omega}$, $\tilde{T}_{\mathrm{L}} = T_{\mathrm{L}}/\mathscr{J} - \hat{T}_{\mathrm{L}}$. It results that $e_\omega = -\tilde{\tilde{\omega}} + \tilde{\omega}$. The correction term v_q in the flux controller (5) is defined using Lyapunov design as explained in Section 4.2.1.

Applying the proposed solution (4)–(9) to the IM model (1), the resulting dynamics of the error variables $(\tilde{T}_{\mathrm{L}}, \tilde{\omega}, e_\omega, \tilde{i}_q, \tilde{\psi}_d, \tilde{\psi}_q, \tilde{i}_d)^{\mathrm{T}}$ is

$$\dot{\tilde{T}}_{\mathrm{L}} = k_{\omega i} e_\omega,$$
$$\dot{\tilde{\omega}} = -k_\omega e_\omega - \tilde{T}_{\mathrm{L}} + \mu\psi^*\tilde{i}_q + \xi_{\varphi 1}, \tag{10}$$

$$\dot{e}_\omega = -k_{io}\tilde{i}_q,$$
$$\dot{\tilde{i}}_q = -k_{iq}\tilde{i}_q - \beta\psi^*(-e_\omega + \tilde{\omega}) + \xi_{\varphi 2}, \tag{11}$$

$$\dot{\tilde{\psi}}_d = -\alpha\tilde{\psi}_d + \omega_2\tilde{\psi}_q + \alpha L_{\mathrm{m}}\tilde{i}_d,$$
$$\dot{\tilde{\psi}}_q = -\alpha\tilde{\psi}_q - \omega_2\tilde{\psi}_d + \psi^*(-e_\omega + \tilde{\omega}) - v_q,$$
$$\dot{\tilde{i}}_d = -k_{id}\tilde{i}_d + \alpha\beta\tilde{\psi}_d + \beta\omega\tilde{\psi}_q, \tag{12}$$

$$\xi_{\varphi 1}(\tilde{\psi}_d, \tilde{\psi}_q, \tilde{i}_d, \tilde{i}_q, \tilde{T}_{\mathrm{L}}, e_\omega, t) = \mu(\tilde{\psi}_d i_q - \tilde{\psi}_q i_d),$$
$$\xi_{\varphi 2}(\tilde{\psi}_d, \tilde{\psi}_q, \tilde{\omega}, t) = \alpha\beta\tilde{\psi}_q - \beta\omega\tilde{\psi}_d, \tag{13}$$

where $\omega_2 = \omega_0 - \omega$ is the slip frequency and $k_{id} = \gamma + k_{id1}$, $k_{iq} = \gamma + k_{iq1}$. The error dynamics is decomposed into three feedback interconnected subsystems: speed tracking (10), speed estimation (11) and flux tracking (12) error dynamics.

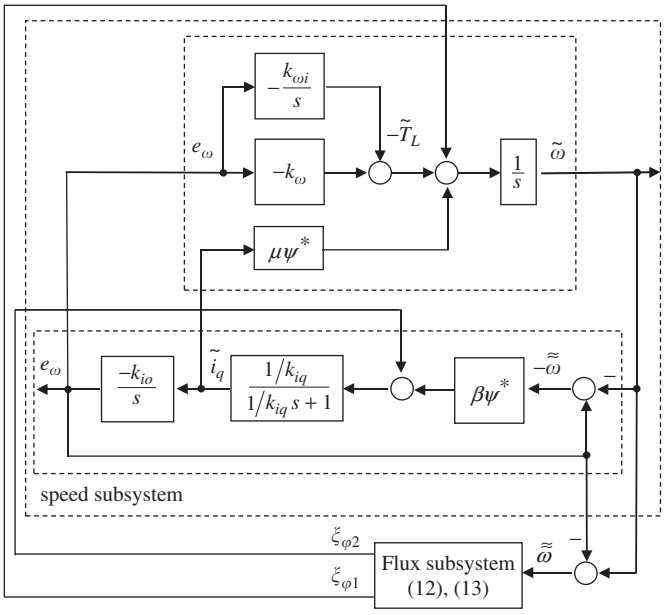


Fig. 1. Block diagram of the speed subsystem.

Remark 1. According to IFO approach, the speed observer and the controller are designed without using explicit flux or current estimation, leading to a simple first-order speed estimation dynamics. The chosen speed estimation law is a part of the q-axis current controller, since the speed estimation error $\tilde{\tilde{\omega}} = -e_\omega + \tilde{\omega}$ directly perturbs the $\tilde{i}_q$ dynamics in (11). This behavior is related to the basic property of field-oriented control, in which the back-EMF term $\beta\psi^*\omega$ appearing in the i_q dynamics is compensated through the torque current controller.

Remark 2. The second order linear filter (11) can be viewed as sensor subsystem for the unmeasurable variable $\tilde{\omega}$. The relevant property of system (10) and (11) is that the nominal speed tracking dynamics (with $\tilde{\psi}_d = \tilde{\psi}_q = \tilde{i}_d = 0$ and $\psi^* = \mathrm{const}$) is linear and can be represented by the block diagram shown in Fig. 1.

Remark 3. An alternative design of the speed estimator, based on the speed dynamics equation in (1), is the following:

$$\dot{\hat{\omega}} = \mu\psi^* i_q^* - \hat{T}_{\mathrm{L}} - k_{io}\tilde{i}_q. \tag{14}$$

This solution would allow to "cancel" all the known terms of the $\tilde{\omega}$ dynamics. As it will be clear in the following, speed estimators (9) and (14) are equivalent in the singular perturbation analysis. Nevertheless, the speed estimator (9) is preferable since it guarantees a unitary static gain between $\tilde{\omega}$ and e_ω (see Fig. 1), while the estimator (14) does not.

Before stating the main result of this paper, the following persistency of excitation (PE) condition is recalled (Khalil, 1996), focusing on a meaningful signal related to the considered problem.

Definition 4. The signal

$$\mathbf{\Omega}(t) = \begin{bmatrix} \Omega_a(t) \\ \Omega_b(t) \end{bmatrix} = \mathrm{e}^{\mathbf{J}\varepsilon_0^{\mathrm{r}}} \begin{bmatrix} \alpha \\ \omega^* \end{bmatrix} = \begin{bmatrix} \alpha\cos\varepsilon_0^{\mathrm{r}} - \omega^*\sin\varepsilon_0^{\mathrm{r}} \\ \alpha\sin\varepsilon_0^{\mathrm{r}} + \omega^*\cos\varepsilon_0^{\mathrm{r}} \end{bmatrix},$$

with $\dot{\varepsilon}_0^{\mathrm{r}} = \omega_0^{\mathrm{r}} = \omega^* + \alpha L_{\mathrm{m}} \frac{i_q^{\mathrm{r}}}{\psi^*}$ and $i_q^{\mathrm{r}} = \frac{1}{\mu\psi^*}\left(\dot{\omega}^* + \frac{T_{\mathrm{L}}}{\mathscr{J}}\right)$, is persistently exciting iff there exist two positive reals T, k such that

$$\int_t^{t+T} \mathbf{\Omega}(\tau)\mathbf{\Omega}^{\mathrm{T}}(\tau)\,\mathrm{d}\tau \geqslant k\mathbf{I}_2 > 0 \quad \text{for all } t \geqslant 0. \tag{15}$$

The properties of the proposed controller with respect to the control objectives (3) are summarized in the following proposition:

Proposition 5. *Considering the system composed of the IM model* (1) *and the controller/observer* (4)–(9), *with* k_{id1}, k_{iq1} *selected such that* $k_{iq} > 0$ *and* $\gamma_1 > 0, k_\omega > 0, k_{io} = (1/2\beta\psi^*)k_{iq}^2$ *and* $k_{\omega i} = k_\omega^2/2$, *if* $\mathbf{\Omega}(t)$ *is persistently exciting, then there exist an* $\varepsilon^* > 0$ *and an invariant set* $\bar{\mathscr{S}} \subseteq \Re^7$ *that contains the origin such that* $\forall \varepsilon \doteq k_\omega/k_{iq} \leqslant \varepsilon^*$ *and for every initial condition of the error variables* $(\tilde{T}_{\mathrm{L}}(0), \tilde{\omega}(0), e_\omega(0), \tilde{i}_q(0), \tilde{\psi}_d(0), \tilde{\psi}_q(0), \tilde{i}_d(0))^{\mathrm{T}} \in \bar{\mathscr{S}}$, *the control objectives* (3) *are guaranteed, with all internal signals bounded.*

4. Stability analysis

In this section the proof of Proposition 5 is given. Stability proof proceeds first by means of proper gain selection in order to impose two-time scale properties to the error dynamics. Then, local exponential stability of the reduced error dynamics is proven. To this purpose, stability of the quasi-steady state flux error dynamics, which represents the crucial property related to PE stated in Definition 4, is investigated separately and then aggregated to speed dynamics. Finally, the overall system stability is proven using standard results for interconnected systems.

4.1. Two-time scale property

The first step of the stability analysis is to define the set of tuning parameters (k_{iq}, k_{io}) for the speed error filter (11) in order to impose that the estimation dynamics (11) is much faster than the speed loop dynamics (10). Define the following linear coordinate transformation for the $\tilde{i}_q$ and e_ω variables: $z_1 = (k_{iq}/2)\tilde{i}_q$, $z_2 = (k_{iq}/2)\tilde{i}_q - \beta\psi^* e_\omega$. Imposing $\varepsilon = k_\omega/k_{iq}$ and selecting k_{io} according to Proposition 5 as $k_{io} = (1/2\beta\psi^*)k_{iq}^2$, error dynamics (10)–(12) become

$$\begin{aligned}
\dot{\tilde{T}}_{\mathrm{L}} &= \frac{k_{\omega i}}{\beta\psi^*}(z_1 - z_2), \\
\dot{\tilde{\omega}} &= -\frac{k_\omega}{\beta\psi^*}(z_1 - z_2) - \tilde{T}_{\mathrm{L}} + \mu\psi^*\frac{2\varepsilon}{k_\omega}z_1 + \xi_{\varphi 1},
\end{aligned} \tag{16}$$

$$\begin{aligned}
\dot{\tilde{\psi}}_d &= -\alpha\tilde{\psi}_d + \omega_2\tilde{\psi}_q + \alpha L_{\mathrm{m}}\tilde{i}_d, \\
\dot{\tilde{\psi}}_q &= -\alpha\tilde{\psi}_q - \omega_2\tilde{\psi}_d + \psi^*\tilde{\omega} - \frac{1}{\beta}(z_1 - z_2) - \upsilon_q,
\end{aligned} \tag{17}$$

$$\begin{aligned}
\dot{\tilde{i}}_d &= -k_{id}\tilde{i}_d + \alpha\beta\tilde{\psi}_d + \beta\omega\tilde{\psi}_q, \\
\varepsilon\dot{z}_1 &= -\frac{k_\omega}{2}z_1 - \frac{k_\omega}{2}z_2 + \frac{k_\omega}{2}(-\beta\psi^*\tilde{\omega} + \xi_{\varphi 2}), \\
\varepsilon\dot{z}_2 &= \frac{k_\omega}{2}z_1 - \frac{k_\omega}{2}z_2 + \frac{k_\omega}{2} \\
&\quad \times (-\beta\psi^*\tilde{\omega} + \xi_{\varphi 2}) - \varepsilon\frac{\dot{\psi}^*}{\psi^*}(z_1 - z_2).
\end{aligned} \tag{18}$$

Note that the relation between k_{iq} and k_{io} imposes a damping factor equal to $\frac{\sqrt{2}}{2}$ to the nominal estimation dynamics (18).

System (16)–(18) is in standard singular perturbation form (Kokotovic, Khalil, & O'Reilly, 1986)

$$\dot{\mathbf{x}}' = f(\mathbf{x}', \mathbf{z}, t, \varepsilon), \tag{19a}$$

$$\varepsilon\dot{\mathbf{z}} = g(\mathbf{x}', \mathbf{z}, t, \varepsilon), \tag{19b}$$

where $\mathbf{x}' = (\tilde{T}_{\mathrm{L}}, \tilde{\omega}, \tilde{\psi}_d, \tilde{\psi}_q, \tilde{i}_d)^{\mathrm{T}} \in \mathscr{B}'_x \subseteq \Re^5$ denotes the "slow" state vector, $\mathbf{z} = (z_1, z_2)^{\mathrm{T}} \in \mathscr{B}_z \subseteq \Re^2$ denotes the "fast" state vector, $t \geqslant 0$ and $\varepsilon \in [0, 1)$ represents the small positive perturbation parameter. $\mathscr{B}'_x, \mathscr{B}_z$ are closed and bounded subsets centered at the origin, f and g are smooth and bounded functions, $f(0, 0, t, \varepsilon) = 0$, $g(0, 0, t, \varepsilon) = 0$, $\forall t, \varepsilon$. System (19) is in standard form since the algebraic equation $0 = g(\mathbf{x}', \mathbf{z}, t, 0)$ possesses a unique isolated solution $\bar{\mathbf{z}} = h(\bar{\mathbf{x}}', t)$. In fact, solving the fast dynamics (18) with $\varepsilon = 0$, the quasi-steady state for $\mathbf{z}$ is obtained as

$$h(\bar{\mathbf{x}}', t) = \begin{pmatrix} \bar{z}_1 \\ \bar{z}_2 \end{pmatrix} = \begin{pmatrix} 0 \\ \xi_{\varphi 2} - \beta\psi^*\tilde{\omega} \end{pmatrix}. \tag{20}$$

Remark 6. From definition of (z_1, z_2) it follows that the solution (20) corresponds to quasi-steady state values for $\tilde{i}_q$ and e_ω given by

$$\bar{\tilde{i}}_q = 0, \quad \bar{e}_\omega = \tilde{\omega} + \frac{1}{\psi^*}(\omega\tilde{\psi}_d - \alpha\tilde{\psi}_q), \tag{21}$$

i.e. the high-gain speed estimation based on back-EMF information is perturbed by the flux tracking errors.

From definition of ε in Proposition 5, it results that for each speed control gain k_ω a suitable k_{iq} can be selected to obtain an arbitrarily small ε, hence the time-scale separation for the full-order error dynamics (16)–(18) can be always imposed.

In order to perform the subsequent steps of the stability analysis reported in next sections, it is imposed that $k_{\omega i} = k_\omega^2/2$ according to Proposition 5 and the following change of coordinates is introduced: $\mathbf{x_m} = (w_1, w_2)^{\mathrm{T}}$ denotes the mechanical error variables, $\mathbf{x_e} = (z_d, z_q, \tilde{i}_d)^{\mathrm{T}}$ denotes the electromagnetic error variables and $\mathbf{y} = (y_1, y_2)^{\mathrm{T}} = \mathbf{z} - h(\mathbf{x}', t)$ denotes the boundary-layer variables, with $w_1 = (k_\omega/2)\tilde{\omega}$, $w_2 = \tilde{T}_{\mathrm{L}} + (k_\omega/2)\tilde{\omega}$, $z_d = \beta\tilde{\psi}_d + \tilde{i}_d$, $z_q = \beta\tilde{\psi}_q$, $y_1 = z_1$, $y_2 = z_2 - \alpha\beta\tilde{\psi}_q + \beta\omega\tilde{\psi}_d + \beta\psi^*\tilde{\omega}$. Substituting (5) in (17), the overall error dynamics (16)–(18) can be rewritten in new variables

as follows:

$$\begin{aligned}\begin{bmatrix}\dot w_1\\ \dot w_2\end{bmatrix} &= k_\omega\begin{bmatrix}-\frac12 & -\frac12\\ \frac12 & -\frac12\end{bmatrix}\begin{bmatrix}w_1\\ w_2\end{bmatrix}\\ &\quad + k_\omega\begin{bmatrix}b_{m1,11}(t,\mathbf{x}_e) & -\frac{z_d-\tilde i_d}{2\beta\psi^*}\\ b_{m1,21}(t,\mathbf{x}_e) & -\frac{z_d-\tilde i_d}{2\beta\psi^*}\end{bmatrix}\begin{bmatrix}w_1\\ w_2\end{bmatrix}\\ &\quad + k_\omega\begin{bmatrix}b_{m2,1}(t,\mathbf{x}_e)\\ b_{m2,2}(t,\mathbf{x}_e)\end{bmatrix}\\ &\quad + k_\omega\begin{bmatrix}\frac{k_\omega(z_d-\tilde i_d)}{2\beta^2\psi^{*2}}\left(\alpha z_q-\omega^*(z_d-\tilde i_d)\right)-\frac{\mu z_q\tilde i_d}{2\beta}\\ \frac{k_\omega(z_d-\tilde i_d)}{2\beta^2\psi^{*2}}\left(\alpha z_q-\omega^*(z_d-\tilde i_d)\right)-\frac{\mu z_q\tilde i_d}{2\beta}\end{bmatrix}\\ &\quad + k_\omega\begin{bmatrix}-\frac{k_\omega}{2\beta\psi^*}\left(1+\frac{z_d-\tilde i_d}{\beta\psi^*}\right)(y_1-y_2)\\ -\frac{k_\omega}{2\beta\psi^*}\frac{z_d-\tilde i_d}{\beta\psi^*}(y_1-y_2)\end{bmatrix}\\ &\quad + \varepsilon\begin{bmatrix}\mu\left(\psi^*+\frac{z_d-\tilde i_d}{\beta}\right)y_1\\ \mu\left(\psi^*+\frac{z_d-\tilde i_d}{\beta}\right)y_1\end{bmatrix}\\ &= \mathbf{A}_m\mathbf{x}_m+\mathbf{B}_{m1}(t,\mathbf{x}_e)\mathbf{x}_m+\mathbf{B}_{m2}(t)\mathbf{x}_e\\ &\quad + \mathbf{B}_{m3}(t,\mathbf{x}_e)\mathbf{x}_e+\mathbf{B}_{m4}(t,\mathbf{x}_e)\mathbf{y}+\mathbf{B}_{m5}(t,\mathbf{x}_e)\mathbf{y}.\end{aligned}\tag{22}$$

$$\begin{aligned}\begin{bmatrix}\dot z_d\\ \dot z_q\\ \dot{\tilde i}_d\end{bmatrix} &= \begin{bmatrix}0 & \omega_0^{\mathrm r} & -\gamma_1\alpha\\ -\omega_0^{\mathrm r} & 0 & -\gamma_1\omega^*\\ \alpha & \omega^* & -(\gamma+\alpha+k_{id1})\end{bmatrix}\begin{bmatrix}z_d\\ z_q\\ \tilde i_d\end{bmatrix}\\ &\quad + \begin{bmatrix}\omega_0^x z_q\\ b_{e1,2}(t,\mathbf{x}_m,\mathbf{x}_e)\\ \frac{2}{k_\omega}w_1 z_q\end{bmatrix}+\begin{bmatrix}\omega_0^y z_q\\ b_{e2,2}(t,\mathbf{x}_e,\mathbf{y})\\ 0\end{bmatrix}\\ &= \mathbf{A}_e(t)\mathbf{x}_e+\mathbf{B}_{e1}(t,\mathbf{x}_m,\mathbf{x}_e)\mathbf{x}_e+\mathbf{B}_{e2}(t,\mathbf{x}_e)\mathbf{y},\end{aligned}\tag{23}$$

$$\begin{aligned}\varepsilon\begin{bmatrix}\dot y_1\\ \dot y_2\end{bmatrix} &= k_\omega\begin{bmatrix}-\frac12 & -\frac12\\ \frac12 & -\frac12\end{bmatrix}\begin{bmatrix}y_1\\ y_2\end{bmatrix}+\varepsilon\begin{bmatrix}0\\ b_{y1,2}(t,\mathbf{x}_m,\mathbf{x}_e,\mathbf{y})\end{bmatrix}\\ &= \mathbf{A}_y\mathbf{y}+\varepsilon\mathbf{B}_{y1}(t,\mathbf{x}_m,\mathbf{x}_e,\mathbf{y})\end{aligned}\tag{24}$$

with

$$b_{m1,11} = -\frac{z_d-\tilde i_d}{\beta\psi^*}-\frac{z_d-\tilde i_d}{2\beta\psi^*}-\frac{(z_d-\tilde i_d)^2}{\beta^2\psi^{*2}},$$

$$b_{m1,21} = -\frac{z_d-\tilde i_d}{2\beta\psi^*}-\frac{(z_d-\tilde i_d)^2}{\beta^2\psi^{*2}},$$

$$b_{m2,1} = \frac{k_\omega}{2\beta\psi^*}\left(\alpha z_q-\omega^*(z_d-\tilde i_d)\right)+\frac{z_d-\tilde i_d}{2\beta\psi^*}\left(\frac{T_{\mathrm L}}{\mathscr J}+\dot\omega^*\right)-\frac{\mu z_q}{2\alpha L_{\mathrm m}\beta}(\alpha\psi^*+\dot\psi^*),$$

$$b_{m2,2} = \frac{z_d-\tilde i_d}{2\beta\psi^*}\left(\frac{T_{\mathrm L}}{\mathscr J}+\dot\omega^*\right)-\frac{\mu z_q}{2\alpha L_{\mathrm m}\beta}(\alpha\psi^*+\dot\psi^*),$$

$$\begin{aligned}b_{e1,2}(t,\mathbf{x}_m,\mathbf{x}_e) = &-\omega_0^x z_d-\gamma_1\hat\omega^x\tilde i_d\\ &+\frac{\tilde i_d^2}{\beta\psi^*}(\omega^*+\hat\omega^x)(1+\gamma_1)+\frac{\tilde i_d^2}{\beta\psi^*}\frac{\alpha L_{\mathrm m}}{\psi^*}\\ &\times(i_q^{\mathrm r}+i_q^x)\end{aligned}$$

$$\begin{aligned}b_{e2,2}(t,\mathbf{x}_e,\mathbf{y}) = &-\omega_0^y z_d-y_1+y_2\\ &-\gamma_1\hat\omega^y\tilde i_d+\frac{\tilde i_d^2}{\beta\psi^*}\hat\omega^y(1+\gamma_1)+\frac{\tilde i_d^2}{\beta\psi^*}\frac{\alpha L_{\mathrm m}}{\psi^*}i_q^y,\end{aligned}$$

$$\begin{aligned}b_{y1,2} = &-\frac{\dot\psi^*}{\psi^*}\left(y_1-y_2+\frac{2\beta\psi^*}{k_\omega}w_1-\xi_{\varphi2}\right)\\ &+\frac{\mathrm d}{\mathrm dt}\left[-\alpha z_q+\left(\omega^*+\frac{2w_1}{k_\omega}\right)(z_d-\tilde i_d)+\frac{2\beta\psi^*}{k_\omega}w_1\right].\end{aligned}$$

Note that in (23) it has been exploited that from definitions (4), (5) it holds $\omega_0\tilde i_d-\beta\upsilon_q=-\gamma_1\hat\omega\tilde i_d+(\upsilon_q/\psi^*)\tilde i_d$. Signals ω_0, $\hat\omega$, i_q have been partitioned into independent time-varying terms, denoted with superscript "r", slow state-dependent terms, dependent on $(t,\mathbf{x}_m,\mathbf{x}_e)$ and denoted with "x", and fast state-dependent terms, dependent on $(t,\mathbf{x}_m,\mathbf{x}_e,\mathbf{y})$ and denoted with "y". Expressions of these terms in (22)–(24) are reported in Appendix A.

Remark 7. Design of the correction term υ_q is instrumental to compensate the flux-dependent perturbing terms in the quasi-steady state value of e_ω in (21) and to define the expression of matrix $\mathbf{A}_e(t)$ given in (23). This result is crucial as enlightened in the Lyapunov analysis reported in Section 4.2.1.

4.2. Stability of the quasi-steady state error dynamics

The quasi-steady state system obtained from (22), (23) with $\varepsilon=0$ and $\mathbf{y}=(y_1,y_2)^{\mathrm T}=0$ can be compactly expressed as

$$\dot{\mathbf{x}}_{\mathbf{m}} = \mathbf{A}_m\mathbf{x}_m+\mathbf{B}_{m1}(t,\mathbf{x}_e)\mathbf{x}_m+\mathbf{B}_{m2}(t)\mathbf{x}_e+\mathbf{B}_{m3}(t,\mathbf{x}_e)\mathbf{x}_e,\tag{25}$$

$$\dot{\mathbf{x}}_{\mathbf{e}} = \mathbf{A}_e(t)\mathbf{x}_e+\mathbf{B}_{e1}(t,\mathbf{x}_m,\mathbf{x}_e)\mathbf{x}_e.\tag{26}$$

It is decomposed into two feedback interconnected subsystems: the mechanical error dynamics (25) and the flux error dynamics (26). In the following, stability analysis of the flux subsystem is reported. Then, stability analysis of the quasi-steady state error dynamics and of the full-order system are carried out.

4.2.1. Flux error subsystem

Flux error dynamics (26) has been expressed as a linear time-varying (LTV) dynamics with the external input $\mathbf{B}_{e1}\mathbf{x}_e$ with bilinear (and higher order) properties. Stability properties of the linearization of the quasi-steady state flux error dynamics, given by $\dot{\mathbf{x}}_e=\mathbf{A}_e(t)\mathbf{x}_e$, are studied.

Defining the time-varying coordinate transformation

$$\begin{bmatrix}z_a\\ z_b\end{bmatrix} = \mathrm e^{\mathbf{J}\varepsilon_0^{\mathrm r}}\begin{bmatrix}z_d\\ z_q\end{bmatrix} = \begin{bmatrix}\cos\varepsilon_0^{\mathrm r} & -\sin\varepsilon_0^{\mathrm r}\\ \sin\varepsilon_0^{\mathrm r} & \cos\varepsilon_0^{\mathrm r}\end{bmatrix}\begin{bmatrix}z_d\\ z_q\end{bmatrix},$$

the linearization of (26) is the LTV system expressed in the state variables $(\tilde{i}_d, z_a, z_b)^{\mathrm{T}}$ as

$$\begin{bmatrix} \dot{\tilde{i}}_d \\ \dot{z}_a \\ \dot{z}_b \end{bmatrix} = \begin{bmatrix} -(\gamma+\alpha+k_{id1}) & \Omega_a(t) & \Omega_b(t) \\ -\frac{1}{\alpha}\left(\frac{R_s}{\sigma}+k_{id1}\right)\Omega_a(t) & 0 & 0 \\ -\frac{1}{\alpha}\left(\frac{R_s}{\sigma}+k_{id1}\right)\Omega_b(t) & 0 & 0 \end{bmatrix} \begin{bmatrix} \tilde{i}_d \\ z_a \\ z_b \end{bmatrix}, \quad (27)$$

where $\Omega_a(t)$, $\Omega_b(t)$ and $\varepsilon_0^{\mathrm{r}}$ are introduced in Definition 4 and γ_1 is defined in (6). In order to investigate the stability properties of (27) the following Lyapunov function is considered

$$V_1 = \frac{1}{2}\left[\alpha\left(\frac{R_s}{\sigma}+k_{id1}\right)^{-1}\left(z_a^2+z_b^2\right)+\tilde{i}_d^2\right]. \quad (28)$$

Its derivative along the trajectories of (27) is equal to

$$\dot{V}_1 = -(\gamma+\alpha+k_{id1})\tilde{i}_d^2. \quad (29)$$

Hence, from (27)–(29) it follows that $(\tilde{i}_d, z_a, z_b)$ are bounded for every $t \geqslant 0$. Direct application of Barbalat's Lemma (Khalil, 1996, p. 192) shows that current tracking error $\tilde{i}_d$ tends asymptotically to zero for the LTV system (27).

Remark 8. From these preliminary results the asymptotic stability of the quasi-steady state flux error dynamics (26) cannot be inferred. In the following, it will be shown that exponential stability of the LTV system (27) and hence local exponential stability of the flux dynamics (26) hold if some persistency of excitation conditions are satisfied.

According to assumptions (A.3) and (A.4), T_{L} is bounded and ω^*, $\dot{\omega}^*$ are bounded functions and therefore $\|\boldsymbol{\Omega}(t)\|$ and $\|\dot{\boldsymbol{\Omega}}(t)\|$ are uniformly bounded. If $\boldsymbol{\Omega}(t)$ is persistently exciting (see (4)), from (28), (29) it follows that system (27) is exponentially stable (Narendra & Annaswamy, 1989, pp. 72–75).

It is interesting to get insight on the operating conditions of the IM where persistency of excitation is satisfied. However, a generic theoretical analysis cannot be easily performed. A simplified but insightful formal analysis is reported in Appendix B. It results that, from a practical point of view, the PE condition (15) is satisfied during all the operating conditions of the IM, apart from dc excitation, i.e. with constant orientation of the rotor flux ($\omega_0 = 0$). This condition corresponds to results reported in Canudas De Wit et al. (2000), Ibarra-Rojas et al. (2004) and is related to lack of observability of the speed sensorless controlled IM under dc excitation.

4.2.2. Overall error dynamics

Local stability of the origin of the quasi-steady state error dynamics (25), (26) will be proved by means of the Lyapunov's method.

Assume that the speed and flux error variables of system (25), (26) are inside compact sets centered at the origin, i.e. $\mathbf{x}_e(t) \in \mathscr{B}_e$, $\mathbf{x}_m(t) \in \mathscr{B}_m$, $\forall t$, where $\mathscr{B}_e = \{\mathbf{x} : \|\mathbf{x}\| < b_e\}$ and $\mathscr{B}_m = \{\mathbf{x} : \|\mathbf{x}\| < b_m\}$ and assume that the PE condition (15) is satisfied. From the stability analysis of Section 4.2.1 for the linearization of the quasi-steady state flux dynamics and linear/bilinear properties of the interconnection terms in (22), (23), the slow subsystem (25), (26) has the following properties:

(P1) $\mathbf{A}_m$ is Hurwitz and the Lyapunov equation $\mathbf{A}_m + \mathbf{A}_m^{\mathrm{T}} = -k_\omega \mathbf{I}_2$ holds;
(P2) $\|\mathbf{B}_{m1}(t, \mathbf{x}_e)\mathbf{x}_m\| \leqslant k_\omega k_1 \|\mathbf{x}_e\|\|\mathbf{x}_m\|$ with $0 < k_1 < \infty$, $\forall \mathbf{x}_e \in \mathscr{B}_e$, $\forall \mathbf{x}_m \in \mathscr{B}_m$, $\forall t$;
(P3) $\|\mathbf{B}_{m2}(t)\| \leqslant k_\omega k_2$ with $0 < k_2 < \infty$, $\forall t$;
(P4) $\|\mathbf{B}_{m3}(t, \mathbf{x}_e)\mathbf{x}_e\| \leqslant k_\omega k_3 \|\mathbf{x}_e\|^2$ with $0 < k_3 < \infty$, $\forall \mathbf{x}_e \in \mathscr{B}_e$, $\forall t$;
(P5) The origin of $\dot{\mathbf{x}}_e = \mathbf{A}_e(t)\mathbf{x}_e$ is globally exponentially stable;
(P6) $\|\mathbf{B}_{e1}(t, \mathbf{x}_m, \mathbf{x}_e)\mathbf{x}_e\| < k_4\|\mathbf{x}_e\|^2 + k_5\|\mathbf{x}_e\|\|\mathbf{x}_m\|$, with $0 < (k_4, k_5) < \infty$, $\forall \mathbf{x}_e \in \mathscr{B}_e$, $\forall \mathbf{x}_m \in \mathscr{B}_m$, $\forall t$;

where $\|(\cdot)\|$ is the Euclidean norm of vector or matrix $(\cdot)$. Properties (P1) and (P5) are related to stability of the isolated mechanical and flux subsystems, (P3) expresses the presence of a linear part in the interconnection term $\mathbf{B}_{m2}(t)\mathbf{x}_e$, while (P2), (P4), (P6) are relative to bilinear (and higher order) coupling terms. The bounds reported in (P2), (P3), (P4) and (P6) are uniform in t since the time-dependent references and the load torque are supposed to be bounded.

Properties of the nonlinear dynamics (25), (26) can be enlightened first by a preliminary analysis of the linear approximation of the quasi-steady state error dynamics. The linear approximation of (25), (26) is given by

$$\dot{\mathbf{x}}_m = \mathbf{A}_m\mathbf{x}_m + \mathbf{B}_{m2}(t)\mathbf{x}_e,$$
$$\dot{\mathbf{x}}_e = \mathbf{A}_e(t)\mathbf{x}_e$$

and is composed of the LTI exponentially stable mechanical dynamics and the LTV electromagnetic dynamics, which is exponentially stable if the PE condition is satisfied. Mechanical and electromagnetic linearized dynamics are interconnected in series structure by means of the bounded matrix $\mathbf{B}_{m2}(t)$. Hence, it follows that the linearized dynamics is globally exponentially stable if the PE condition is satisfied.

Utilizing results from Khalil (1996, Theorem 3.11) and Vidyasagar (1978, Section 5.4), it is shown that the origin of the quasi-steady state error dynamics (25), (26) is locally exponentially stable (see Appendix C).

4.3. Full-order error dynamics

Assuming that state variables of the speed, flux and boundary-layer error dynamics are inside compact sets centered at the origin, i.e. $\mathbf{x}_e(t) \in \mathscr{B}_e$, $\mathbf{x}_m(t) \in \mathscr{B}_m$, $\mathbf{y}(t) \in \mathscr{B}_y$, $\forall t$, where $\mathscr{B}_e = \{\mathbf{x} : \|\mathbf{x}\| < b_e\}$, $\mathscr{B}_m = \{\mathbf{x} : \|\mathbf{x}\| < b_m\}$, $\mathscr{B}_y = \{\mathbf{x} : \|\mathbf{x}\| < b_y\}$, and assuming that the PE condition (15) is satisfied, the following properties hold for the full-order error dynamics (22)–(24) in addition to properties P1–P6:

(P7) $\|\mathbf{B}_{m4}(t, \mathbf{x}_e)\| \leqslant k_\omega k_6$ with $0 < k_6 < \infty$, $\forall \mathbf{x}_e \in \mathscr{B}_e$, $\forall t$;
(P8) $\|\mathbf{B}_{m5}(t, \mathbf{x}_e)\| \leqslant \varepsilon k_7$ with $0 < k_7 < \infty$, $\forall \mathbf{x}_e \in \mathscr{B}_e$, $\forall t$;
(P9) $\|\mathbf{B}_{e2}(t, \mathbf{x}_e)\| \leqslant k_8$ with $0 < k_8 < \infty$, $\forall \mathbf{x}_e \in \mathscr{B}_e$, $\forall t$;
(P10) $\mathbf{A}_y$ is Hurwitz and the Lyapunov equation $\mathbf{A}_y + \mathbf{A}_y^{\mathrm{T}} = -k_\omega \mathbf{I}_2$ holds;

(P11) $\|\mathbf{B}_{y1}(t, \mathbf{x}_m, \mathbf{x}_e, \mathbf{y})\| \leqslant (k_9 + k'_9/k_\omega)\|\mathbf{x}_m\| + k_{10}\|\mathbf{x}_e\| + (k_{11} + \varepsilon k'_{11}/k_\omega)\|\mathbf{y}\|$ with $0 < (k_9, k'_9, k_{10}, k_{11}, k'_{11}) < \infty$, $\forall \mathbf{x}_m \in \mathscr{B}_m$, $\forall \mathbf{x}_e \in \mathscr{B}_e$, $\forall \mathbf{y} \in \mathscr{B}_y$, $\forall t$.

Note that properties P7–P9 and P11 establish the presence of linear parts in the coupling terms dependent on fast variables $\mathbf{y}$. From properties (P1)–(P11), local uniform asymptotic stability of the origin of the full-order error dynamics (22)–(24) turns out. The stability analysis, which follows the same steps of the proof of Appendix C, and the evaluation of ε^* (see Proposition 5) are based on standard methods for singularly perturbed systems with exponentially stable reduced and boundary-layer subsystems (Khalil, 1996, Chapter 9). Estimate of the domain of attraction is based on classical Lyapunov-like technique (Khalil, 1996, Chapter 4). Stability proof is not reported here for the sake of space. Since $\mathbf{x}_e(t), \mathbf{x}_m(t), \mathbf{y}(t)$ tend exponentially to zero, provided that initial conditions are inside the domain of attraction, it follows that asymptotic speed and rotor flux modulus tracking together with field orientation are achieved.

5. Experimental results

The proposed sensorless control algorithm has been experimentally tested using a two pole pairs 1.1 kW standard induction motor, with 7.0 Nm rated torque and 1410 rev/ min rated speed at 50 Hz. Motor data are the following: rated voltage is 220 V, rated current is 2.8 A, excitation current is 1.4 A, stator and rotor resistances are $R_s = 10.4\,\Omega$, $R_r = 4.5\,\Omega$, magnetization inductance is $L_m = 0.434$ H, stator and rotor inductances are $L_s = L_r = 0.47$ H, total inertia is $\mathscr{J} = 0.0034\,\mathrm{Kg\,m^2}$.

5.1. Controller tuning

The sensorless controller defined in (4)–(9) generates the error dynamics given by (16)–(18). Parameters tuning is strictly related to the structure of the error dynamics. Control parameters of the flux subsystem (17) are the proportional d-axis current controller gain k_{id1} and the correction gain γ_1, linked by relation (6). According to tuning relations in Proposition 5 between the speed controller proportional and integral gains $k_\omega, k_{\omega i}$ and between the proportional gain k_{iq1} of the q-axis current regulator and the speed estimator gain k_{io}, the second order nominal speed error dynamics in (22) and the fast second order nominal error dynamics (18) are characterized by a time-constant equal to $\tau_\omega = \sqrt{2}/k_\omega$ and $\tau_o = \sqrt{2}/k_{iq}$, respectively, with damping factor equal to $\delta = \sqrt{2}/2$. Two-time-scale separation in system (16)–(18) is practically achieved with $\tau_o \leqslant (\frac{1}{4}$ to $\frac{1}{2})\tau_\omega$, i.e. with $\varepsilon \leqslant (\frac{1}{4}$ to $\frac{1}{2})$. During all the tests the controller parameters are set at constant values $k_{id1} = 300$, $\gamma_1 = 47$, $k_\omega = 140$, $k_{\omega i} = 9800$, $k_{iq1} = 160$, while, according to tuning relation in Proposition 5 and considering $p = 2$ pole pairs, k_{io} is selected as $k_{io} = (1/2p\beta\psi^*)k_{iq}^2 = 2870$ when constant rated reference flux is $\psi^* = 0.86$ Wb.

5.2. Operating sequences

The flux and speed reference trajectories adopted in the experiments are presented in Fig. 2 using solid lines; dashed line in the same figure represents the load torque profile. The operating sequence of the performed tests is the following:

(A) The machine is excited during the initial time interval 0–0.096 s using a flux reference trajectory starting at $\psi^*(0) = 0.02$ Wb and reaching the motor rated value of 0.86 Wb with the first and second derivatives equal to 10 Wb/s and 1000 Wb/s^2, correspondingly.
(B) The unloaded motor is required to track the speed reference trajectory characterized by the following phases: starting from $t = 0.4$ s with zero initial value, speed reference trajectory reaches 100 rad/s at $t = 0.45$ s; from this time up to $t = 1.3$ s constant speed is imposed; from $t = 1.3$ s the motor is required to stop at zero speed reference. Maximum absolute values of the first and second derivatives of the speed reference trajectory are equal to 2200 rad/s^2 and 20 000 rad/s^3, correspondingly. Tracking of the speed reference trajectory requires rated motor torque.
(C) From time $t = 0.7$ s to $t = 1.0$ s a constant load torque, equal to 100% of the motor rated value (7.0 Nm), is applied.

Remark 9. The reference trajectories, controllers' initialization and sequence of motor operation must be properly specified in order: (a) not to violate physical constraints of motor operations; (b) to guarantee small enough initial flux errors in correspondence with local stability properties; (c) to achieve specified tracking performance. According to previous

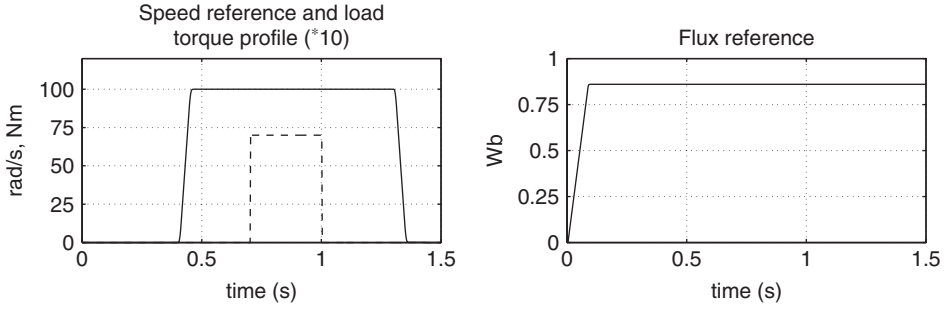


Fig. 2. Speed, flux references and load torque profile (dashed line).

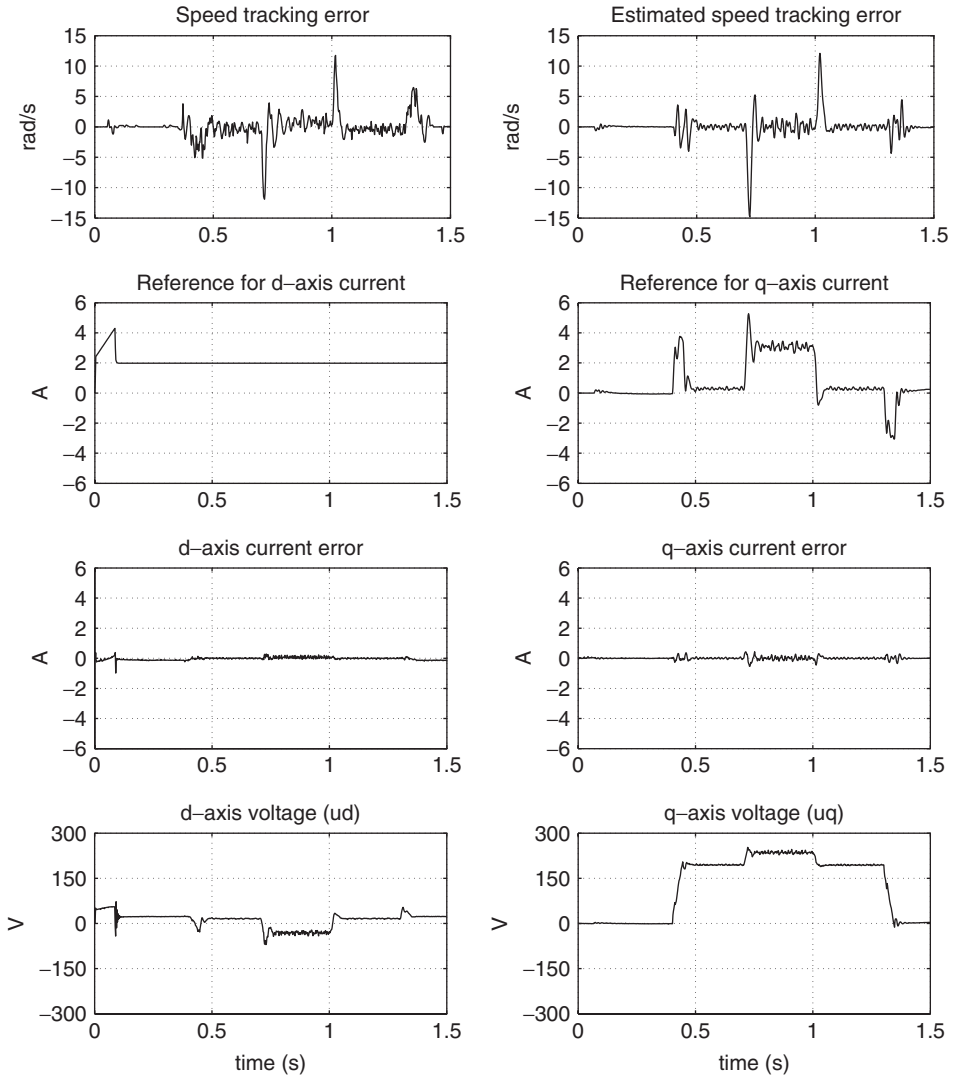


Fig. 3. Experimental results: dynamic behavior of the sensorless controller with maximum speed reference equal to 100 rad/s and applied load torque equal to 7.0 Nm.

considerations, with the initial excitation stage torque production starts when flux tracking errors are negligible, leading to accurate speed estimation (21). In this case, the only significant perturbation for system is load torque variation, since large step-wise load torque is applied.

5.3. Experimental set-up

The experimental tests have been carried out using a rapid prototyping station, which includes a Personal Computer acting as the Operator Interface during the experiments, a custom floating-point digital signal processor board based on TMS320C32 and a 50 A/380 V_{RMS} three-phase inverter to feed the adopted IM. A symmetrical three-phase PWM technique with 10 kHz switching frequency has been used to control the inverter. A vector controlled permanent magnet synchronous motor has been used to provide the load torque.

In the rapid prototyping station, two stator phase currents are measured by Hall-effect zero-field sensors. Only for monitoring purposes, the motor speed is measured by means of a 512 pulse/revolution incremental encoder.

The sampling time for the controller has been set to 200 μs. In order to get the discrete-time version of control algorithm the simple Euler method has been used.

5.4. Experimental and simulation results

A first set of experiments, whose results are reported in Fig. 3, has been performed in order to test the dynamic performance of the control algorithm during speed trajectory tracking and load torque rejection at high speed. The transient performance is characterized by a maximum speed tracking error of about 5 rad/s during speed reference variation and about 12 rad/s during load torque rejection transients. Steady-state

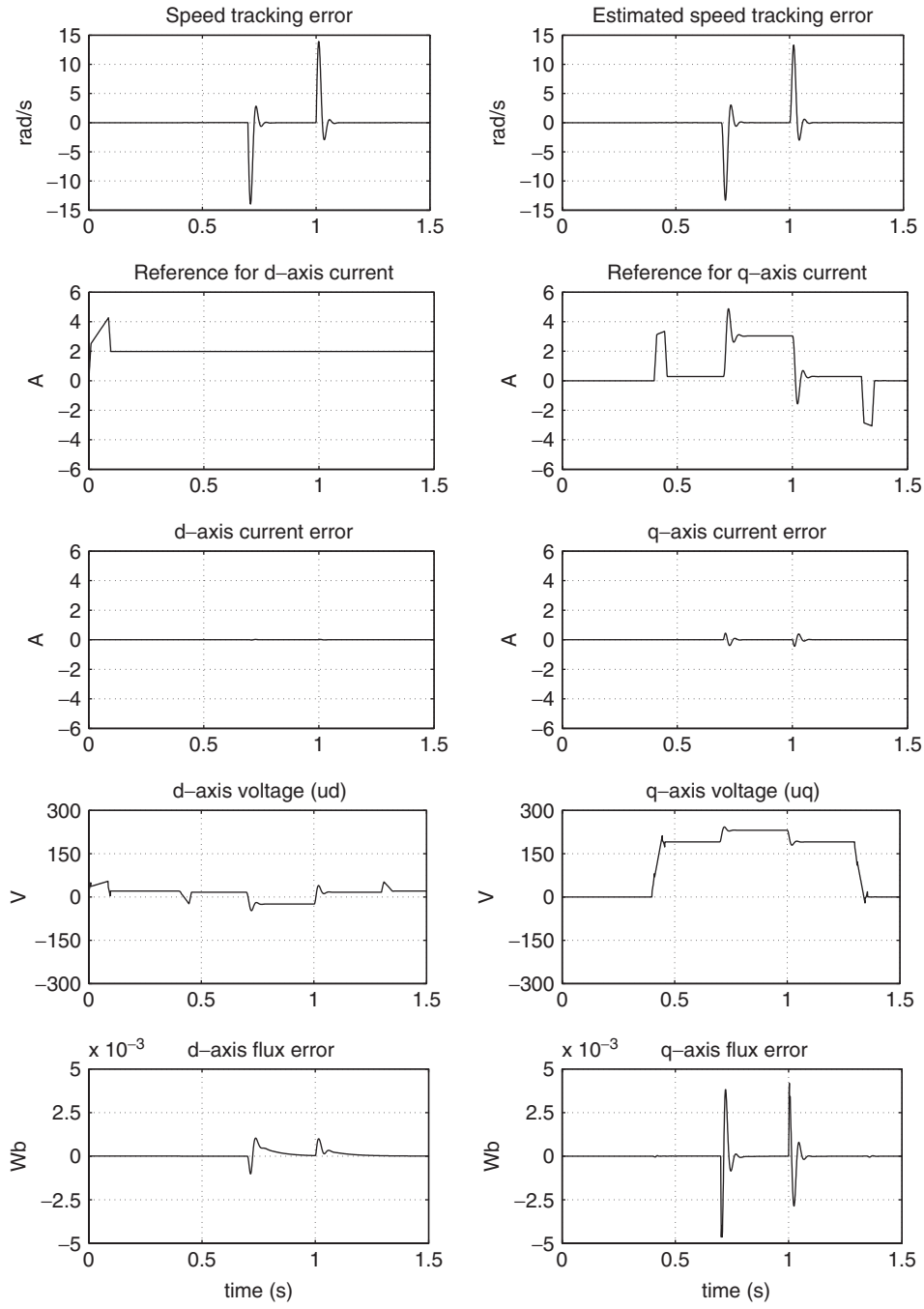


Fig. 4. Simulation results: dynamic behavior of the sensorless controller.

speed tracking error is almost zero when constant reference speed and constant load torque are imposed. Estimated speed tracking error is close to the actual one even during transients, confirming that time-scale separation is achieved. Negligible current regulation errors are present during the experiments.

To validate the controller performance during experimental tests, comparison with simulation has been performed, under the same operating conditions of Fig. 2. In order to take into account the mechanical friction present in the experimental set-up, a linear friction torque $-(v/\mathcal{J})\omega$ is added in the simulated IM model and compensated with feed-forward actions in the controller. Friction coefficient value is $v = 0.0068\,\mathrm{Nm/(rad/s)}$. Simulation results, reported in Fig. 4, are similar to the experimental results in Fig. 3. The same maximum amplitude of both estimated and actual speed tracking error is obtained during load torque rejection. Note that in simulation tests, zero speed tracking error is achieved during steady-state conditions and during speed reference variation, while speed tracking error is not null in the experiments. This is mainly due to IM parameters uncertainties and inverter non-idealities such as dead-time

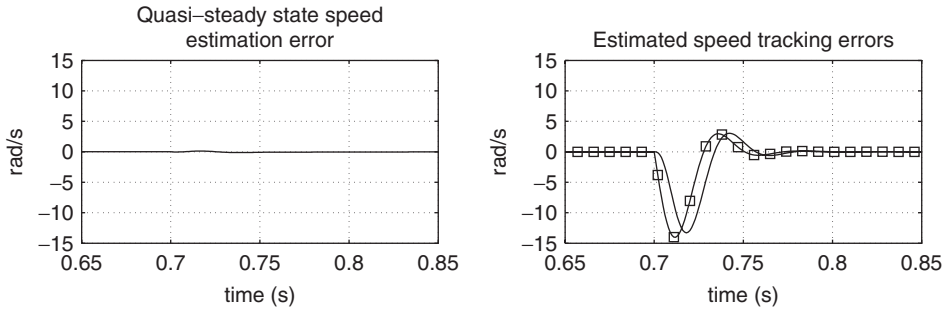


Fig. 5. Simulation results: load torque transient. Speed estimation error $\tilde{\omega} - \bar{e}_\omega$. Estimated speed tracking error e_ω (solid) and $\bar{e}_\omega$ (marked).

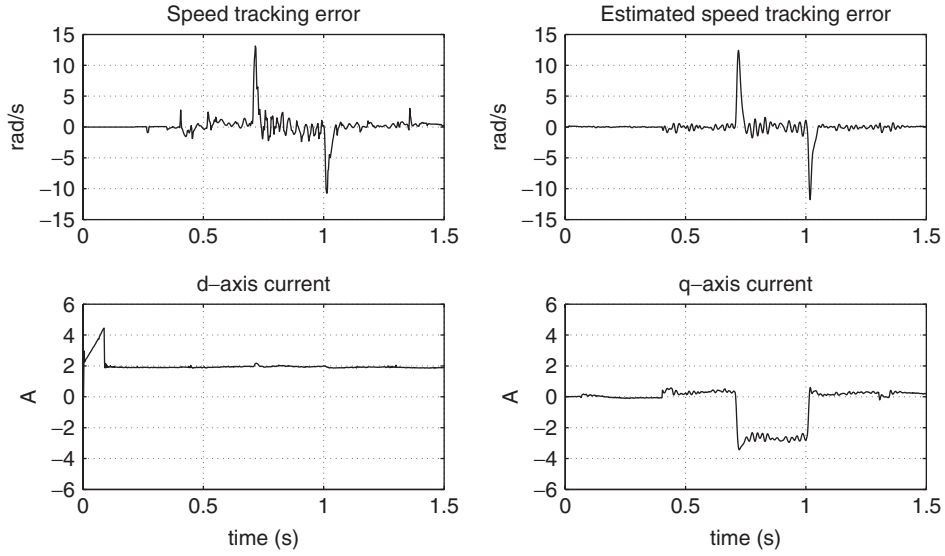


Fig. 6. Experimental results: dynamic behavior of the sensorless controller with maximum speed reference equal to 10 rad/s and applied regenerative torque equal to −7.0 Nm.

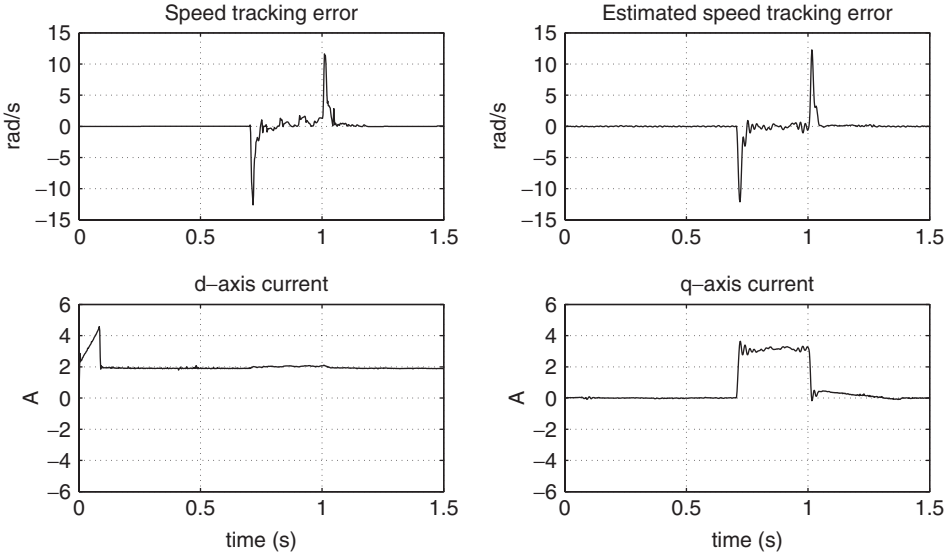


Fig. 7. Experimental results: dynamic behavior of the sensorless controller with zero speed reference ($\omega^* = 0$ rad/s).

effect and voltage commutations. Stator current and voltage profiles during experimental and simulation tests are comparatively shown in Figs. 3 and 4. In Fig. 4 rotor flux errors are also reported, showing that asymptotic flux amplitude regulation and field orientation are achieved.

In Fig. 5 the behavior of $\tilde{\omega}-\bar{e}_\omega$, e_ω and $\bar{e}_\omega$ defined in (21) is reported. A zoom of the first load torque transient is considered. From the first picture it can be noted that $\tilde{\omega}-\bar{e}_\omega$ is very small compared to $\tilde{\omega}$ and e_ω in Fig. 4, hence the quasi-steady state behavior of e_ω is very similar to $\tilde{\omega}$ and the contribution related to flux errors (see (21)) is almost negligible. In the second picture of Fig. 5 the similarity between the actual variable e_ω and its quasi-steady state version $\bar{e}_\omega$ is enlightened, confirming the established time-scale separation.

A second set of experiments has been performed to test the proposed solution when the PE condition (15) fails or is near to fail. As it is well-known in the application-oriented literature (Rajashekara et al., 1996) and according to the analysis in Section 4.2.1 and Appendix B, the condition $\omega_0 = 0$ is critical and particularly significant in real-world applications.

In Fig. 6 a low-speed, regenerative condition (i.e. with negative output mechanical power) is considered. A speed reference profile with shape similar to Fig. 2, maximum speed of 10 rad/s and maximum time derivative of 220 rad/s^2 has been imposed; -7.0 Nm regenerative torque is applied following the operating sequence of Section 5.2. The nominal ω_0 is very close to zero with regenerative torque (ω_0=5.9 rad/s). No significant performance degradation is present in low-speed regenerative-torque condition (Fig. 6) with respect to tests at high-speed (Fig. 3).

In Fig. 7 rejection of the rated load torque with zero speed reference is considered according to the operating sequence of Section 5.2. In this experiment nominal ω_0 goes from zero to 14.1 rad/s and back. Again, the performances are very similar to previous cases; only after the load torque step down a small residual speed error can be noted, owing to lack of PE.

Results of experimental tests confirm that the achievable dynamic performances of the speed sensorless controller are comparable to those obtained with high performance vector controlled induction motor drives with speed measurement, for typical operating conditions including zero speed and regenerative mode.

6. Conclusions

It has been proven that the proposed speed-sensorless controller guarantees local asymptotic tracking of smooth speed and flux references along with asymptotic field orientation, with constant unknown load torque, if the estimation dynamics is imposed to be sufficiently faster than the speed/flux one and if a persistency of excitation condition is satisfied. As far as the latter is concerned, essentially a non-null synchronous frequency is required. This condition is well established in both methodological and application-oriented literature; future efforts will be devoted to avoid this condition without impairing the control performances.

Since the stability analysis invokes the converse Lyapunov theorem and an integral PE condition, the existence of the small positive real ε^* and the domain of attraction $\bar{\mathscr{S}}$ is proved, without providing their evaluation. A constructive procedure for controller parameters selection is obtained from the controller design. This procedure is conceptually similar to that one adopted in industrial drives, thanks to cascaded structure of the overall system dynamics with established time-scale properties for control loops. Moreover, the physically-based structure of the controller leads to a straightforward simplification if rotor speed is measured.

Experiments and simulations in typical operating conditions demonstrate high dynamic performance during speed and flux tracking including load torque rejection, which is of the same order as for standard field-oriented solutions with speed measurement.

Appendix A. Definitions

$$\hat{\omega} = \omega^*(t) + \hat{\omega}^x(t, \mathbf{x}_m, \mathbf{x}_e) + \hat{\omega}^y(t, \mathbf{x}_m, \mathbf{x}_e, \mathbf{y}),$$
$$\hat{\omega}^x = \frac{1}{\beta\psi^*}\left[-\alpha z_q + \left(\omega^* + \frac{2}{k_\omega}w_1\right)(z_d - \tilde{i}_d) + \frac{2}{k_\omega}\beta\psi^* w_1\right],$$
$$\hat{\omega}^y = \frac{1}{\beta\psi^*}(y_1 - y_2),$$

$$i_q = i_q^{\mathrm{r}}(t) + i_q^x(t, \mathbf{x}_m, \mathbf{x}_e) + i_q^y(t, \mathbf{x}_m, \mathbf{x}_e, \mathbf{y}),$$
$$i_q^{\mathrm{r}} = \frac{1}{\mu\psi^*}\left[\dot{\omega}^* + \frac{T_{\mathrm{L}}}{\mathscr{J}}\right]; \quad i_q^y = \frac{2\varepsilon}{k_\omega}y_1 - \frac{k_\omega}{\mu\psi^*}\frac{1}{\beta\psi^*}(y_1 - y_2),$$
$$i_q^x = \frac{1}{\mu\psi^*}(w_1 - w_2) + \frac{k_\omega}{\mu\psi^*}\frac{1}{\beta\psi^*} \times \left[\alpha z_q - \left(\omega^* + \frac{2}{k_\omega}w_1\right)(z_d - \tilde{i}_d) - \frac{2}{k_\omega}\beta\psi^* w_1\right],$$

$$\omega_0 = \omega_0^{\mathrm{r}}(t) + \omega_0^x(t, \mathbf{x}_m, \mathbf{x}_e) + \omega_0^y(t, \mathbf{x}_m, \mathbf{x}_e, \mathbf{y}),$$
$$\omega_0^{\mathrm{r}} = \omega^* + \alpha L_{\mathrm{m}}\frac{i_q^{\mathrm{r}}}{\psi^*}; \quad \omega_0^x = \hat{\omega}^x + \alpha L_{\mathrm{m}}\frac{i_q^x}{\psi^*} + \frac{1}{\beta\psi^*}(1+\gamma_1)(\omega^* + \hat{\omega}^x)\tilde{i}_d + \frac{1}{\beta\psi^*}\frac{\alpha L_{\mathrm{m}}}{\psi^*}\left(i_q^{\mathrm{r}} + i_q^x\right)\tilde{i}_d,$$
$$\omega_0^y = \hat{\omega}^y + \alpha L_{\mathrm{m}}\frac{i_q^y}{\psi^*} + \frac{1}{\beta\psi^*}(1+\gamma_1)\hat{\omega}^y\tilde{i}_d + \frac{1}{\beta\psi^*}\frac{\alpha L_{\mathrm{m}}}{\psi^*}i_q^y\tilde{i}_d.$$

Appendix B. Persistency of excitation

To enlighten when persistency of excitation is guaranteed for the electromagnetic dynamics, assume for simplicity steady-state conditions for the reference speed and for the reference frame angular speed, i.e. constant steady-state conditions for $\omega^*, \psi^*, T_{\mathrm{L}}$. Supposing $\omega_0^{\mathrm{r}} = \text{const} \neq 0$ and $\omega^* = \text{const}$, and choosing $T = 2\pi/|\omega_0^{\mathrm{r}}|$, the PE condition (15) becomes $\int_t^{t+T}\mathbf{\Omega}(\tau)\mathbf{\Omega}(\tau)^{\mathrm{T}}\mathrm{d}\tau = \mathrm{diag}((\alpha^2+\omega^{*2})\pi/|\omega_0^{\mathrm{r}}|, (\alpha^2+\omega^{*2})\pi/|\omega_0^{\mathrm{r}}|) > \alpha^2\pi/|\omega_0^{\mathrm{r}}|$, hence choosing $k = \alpha^2\pi/|\omega_0^{\mathrm{r}}|$, if $\omega_0^{\mathrm{r}} \neq 0$ the PE condition is satisfied.

On the other hand, assuming $\omega_0^{\mathrm{r}} = 0$ (and $\varepsilon_0^{\mathrm{r}} = 0$ without loss of generality) during time interval $[t, t+T]$, with $T > 0$, and considering a generic reference speed $\omega^*(t)$, the PE condition

(15) becomes

$$\int_t^{t+T} \mathbf{\Omega}(\tau)\mathbf{\Omega}^{\mathrm{T}}(\tau)\,\mathrm{d}\tau = \begin{bmatrix} \int_t^{t+T} \alpha^2\,\mathrm{d}\tau & \int_t^{t+T} \alpha\omega^*(\tau)\,\mathrm{d}\tau \\ \int_t^{t+T} \alpha\omega^*(\tau)\,\mathrm{d}\tau & \int_t^{t+T} \omega^{*2}(\tau)\,\mathrm{d}\tau \end{bmatrix}.$$

Applying Cauchy–Schwartz–Buniakowsky theorem, it follows that the PE condition is satisfied if $\omega_0^{\mathrm{r}}=0$ and $\omega^*(t)$ is not constant during the time interval $[t, t+T]$. Actually this condition is not meaningful from a practical viewpoint. On the other side, PE is not satisfied with constant ω^* and $\omega_{0\mathrm{r}}=0$, i.e. during regenerative condition with dc excitation.

Appendix C. Stability proof of the origin of the quasi-steady state system

Recalling property P5 and applying the converse Lyapunov theorem (Khalil, 1996, Theorem 3.12) for exponentially stable systems to the linear approximation of the flux error dynamics (26), it follows that there exist positive constants c_1, c_2, c_3, c_4 and a function $V_e(t, \mathbf{x}_e)$ such that $c_1\|\mathbf{x}_e\|^2 \leqslant V_e(t, \mathbf{x}_e) \leqslant c_2\|\mathbf{x}_e\|^2$, $(\partial V_e/\partial \mathbf{x}_e)\mathbf{A}_e(t)\mathbf{x}_e + \partial V_e/\partial t < -c_3\|\mathbf{x}_e\|^2$, $\|\partial V_e/\partial \mathbf{x}_e\| < c_4\|\mathbf{x}_e\|$. Consider the candidate Lyapunov function $V = \frac{1}{2}\mathbf{x}_m^{\mathrm{T}}\mathbf{x}_m + \delta V_e(t, \mathbf{x}_e)$ where $\delta > 0$ is a constant positive gain to be designed. Recalling properties P1–P4, its time derivative along the trajectories of (25), (26) is $\dot{V} \leqslant -k_\omega/2\|\mathbf{x}_m\|^2 + k_\omega k_1\|\mathbf{x}_e\|\|\mathbf{x}_m\|^2 - \delta c_3\|\mathbf{x}_e\|^2 + \delta c_4 k_4\|\mathbf{x}_e\|^3 + k_\omega k_2\|\mathbf{x}_e\|\|\mathbf{x}_m\| + (k_\omega k_3 + \delta c_4 k_5)\|\mathbf{x}_e\|^2\|\mathbf{x}_m\|$. Applying Young's inequalities $2ab \leqslant ka^2 + b^2/k$, with $a, b \in \Re$, $k \in (0, 1)$ to the last two terms, the following inequalities hold: $k_\omega k_2\|\mathbf{x}_e\|\|\mathbf{x}_m\| \leqslant k_\omega/4\|\mathbf{x}_m\|^2 + k_\omega k_2^2\|\mathbf{x}_e\|^2$, $(k_\omega k_3 + \delta c_4 k_5)\|\mathbf{x}_e\|^2\|\mathbf{x}_m\| \leqslant k_\omega k_3 + \delta c_4 k_5/2\|\mathbf{x}_e\|\|\mathbf{x}_m\|^2 + k_\omega k_3 + \delta c_4 k_5/2\|\mathbf{x}_e\|^3$. Hence, it follows that $\dot{V} \leqslant -[k_\omega/4 - [k_\omega(k_1+k_3/2)+\delta c_4 k_5/2]\|\mathbf{x}_e\|]\|\mathbf{x}_m\|^2 - [\delta c_3 - k_\omega k_2^2 - [k_\omega k_3/2 + \delta c_4(k_4 + k_5/2)]\|\mathbf{x}_e\|]\|\mathbf{x}_e\|^2$. Choosing $\delta = 2k_\omega k_2^2/c_3$ it holds $\dot{V} \leqslant -k_\omega[\frac{1}{4} - (k_1 + k_3/2 + c_4 k_5 k_2^2/c_3)\|\mathbf{x}_e\|]\|\mathbf{x}_m\|^2 - k_\omega[k_2^2 - (k_3/2 + 2k_2^2 c_4/c_3(k_4 + k_5/2))\|\mathbf{x}_e\|]\|\mathbf{x}_e\|^2$, $\forall \|\mathbf{x}_e\| \leqslant b_e, \forall \|\mathbf{x}_m\| \leqslant b_m$. Imposing that $\|\mathbf{x}_e(t)\| \leqslant L_e, \forall t$, where $L_e = \min\{b_e, \frac{1}{8}(k_1 + k_3/2 + c_4 k_5 k_2^2/c_3)^{-1}, \frac{1}{2}k_2^2(k_3/2 + 2k_2^2 c_4/c_3(k_4 + k_5/2))^{-1}\}$, the following inequality holds: $\dot{V} \leqslant -k_\omega/8\|\mathbf{x}_m\|^2 - k_\omega k_2^2/2\|\mathbf{x}_e\|^2$, $\forall \|\mathbf{x}_e(t)\| < L_e, \forall \|\mathbf{x}_m(t)\| < b_m$. Hence, the origin of system (25), (26) is locally exponentially stable.

References

Canudas De Wit, C., Youssef, A., Barbot, J. P., Martin, P. & Malrait, F. (2000). Observability conditions of induction motors at low frequencies. In *Proceedings of the 39th IEEE conference on decision and control* (Vol. 3, pp. 2044–2049). Sydney, Australia.

Chern, T., Chang, J., & Tsai, K. (1998). Integral-variable-structure-control-based adaptive speed estimator and resistance identifier for induction motor. *International Journal of Control*, *69*(1), 31–47.

Doki, S., Sangwongwanick, S. & Okuma, S. (1992). Implementation of speed-sensor-less field oriented vector control using adaptive sliding observer. In *Proceedings of the 18th IEEE conference on industrial electronics* (pp. 453–458). San Diego, CA.

Feemster, M., Aquino, P., Dawson, D. M., & Behal, A. (2001). Sensorless rotor velocity tracking control for induction motors. *IEEE Transactions on Control Systems Technology*, *9*(4), 645–653.

Holtz, J. (2002). Sensorless control of induction motor drives. *Proceedings of the IEEE*, 90(8), 1359–1394.

Ibarra-Rojas, S., Moreno, J., & Espinosa-Perez, G. (2004). Global observability analysis of sensorless induction motors. *Automatica*, *40*(6), 1079–1085.

Khalil, H. K. (1996). *Nonlinear systems*. (2nd ed.), Upper Saddle River, NJ: Prentice Hall.

Kokotovic, P. V., Khalil, H. K., & O'Reilly, J. (1986). *Singular perturbation methods in control: Analysis and design*. London: Academic Press.

Kubota, H., & Matsuse, K. (1994). Speed sensorless field-oriented control of induction motor with rotor resistance adaptation. *IEEE Transactions on Industry Applications*, *30*(5), 1219–1224.

Leonhard, W. (2001). *Control of electrical drives*. (3rd ed.), Berlin: Springer.

Marino, R., Tomei, P. & Verrelli, C. M. (2002a). Adaptive control of sensorless induction motors with uncertain rotor resistance. In *Proceedings of the 41st IEEE conference on decision and control* (pp. 148–153). Las Vegas, Nevada.

Marino, R., Tomei, P. & Verrelli, C. M. (2002b). A new global control scheme for sensorless current-fed induction motors. In *15th IFAC triennial world congress*, Barcelona, Spain.

Marino, R., Tomei, P., & Verrelli, C. M. (2004a). A global tracking control for speed-sensorless induction motors. *Automatica*, *40*(6), 1071–1077.

Marino, R., Tomei, P. & Verrelli, C. M. (2004b). Nonlinear tracking control for sensorless induction motors. In *Proceedings of the 43rd IEEE conference on decision and control*. Paradise Island, Bahamas.

Montanari, M., Peresada, S. & Tilli, A. (2003). Sensorless control of induction motors with exponential stability property. In *Proceedings of the 2003 European control conference*. Cambridge, UK.

Montanari, M., Peresada, S. & Tilli, A. (2004). Sensorless control of induction motor with adaptive speed-flux observer. In *Proceedings of the 43rd IEEE conference on decision and control*. Paradise Island, Bahamas.

Montanari, M., Peresada, S., Tilli, A. & Tonielli, A. (2000). Speed sensorless control of induction motor based on indirect field-orientation. In *Proceedings of the 35th IEEE conference on industry application*, Rome, Italy.

Narendra, K. S., & Annaswamy, A. M. (1989). *Stable adaptive systems*. Englewood Cliffs, NJ: Prentice-Hall.

Peng, F., & Fukao, T. (1994). Robust speed identification for speed-sensorless vector control of induction motors. *IEEE Transactions on Industry Applications*, *30*(5), 1234–1240.

Peresada, S., Montanari, M., Tilli, A. & Kovbasa, S. (2002). Sensorless indirect field-oriented control of induction motors, based on high gain speed estimation. In *Proceedings of the 28th IEEE conference on industrial electronics*. Sevilla, Spain.

Peresada, S., & Tonielli, A. (2000). High-performance robust speed-flux tracking controller for induction motor. *International Journal of Adaptive Control and Signal Processing*, *14*, 177–200.

Rajashekara, K., Kawamura, A., & Matsuse, K. (1996). *Sensorless control of AC motor drives*. New York: IEEE Press.

Schauder, C. (1992). Adaptive speed identification for vector control of induction motors without rotational transducers. *IEEE Transactions on Industry Applications*, *28*(5), 1054–1061.

Vas, P. (1998). *Sensorless vector and direct torque control*. Oxford: Oxford University Press.

Vidyasagar, M. (1978). *Nonlinear systems analysis*. Englewood Cliffs, NJ: Prentice-Hall.

Yan, Z., Jin, C. & Utkin, V.I. (2000). Sensorless sliding-mode control of induction motors. *IEEE Transactions on Industrial Electronics* 47 (6).



Marcello Montanari was born in Ravenna, Italy, in 1974. He received the Dr. Ing. degree in computer science engineering and the Ph.D. degree in Automatic Control at the University of Bologna, Italy, in 1999 and 2003, respectively. Since 2003, he has a Post-Doc position within the Department of Electronics, Computer Science and Systems, University of Bologna. His current research interests include applied nonlinear and adaptive control, in the field of electric drives, automotive applications, electro-mechanical and electro-hydraulic systems.



Sergei M. Peresada was born in 1952, Donetsk, USSR. He received the Diploma of Electrical Engineer from the Donetsk Polytechnic Institute in 1974 and the Candidate of Technical Sciences degree (corresponding to Ph.D.) in control and automation from the Kiev Polytechnic Institute in 1983. He has been working at the Department of Electrical Engineering and Automation of the National Technical University of Ukraine "Kiev Polytechnic Institute" since 1977, where he is currently Professor of Control and Automation. He has been Visiting Professor at the University of Illinois (Urbana-Champaign), University of Rome Tor Vergata, DEIS and Institute of Advanced Study University of Bologna. He currently serves as Associate Editor of the IEEE Transactions on Control Systems Technology.

His research interests include nonlinear and adaptive control of electromechanical systems based on AC motors, control of power converters. He is author of about 150 scientific publications and co-author of the volumes: "Theory and Control of Electrical Drives" and "Control of Electromechanical Systems".



Andrea Tilli was born in Bologna, Italy, on April 4, 1971. He received the Dr. Ing. degree in electronic engineering from the University of Bologna, Italy, in 1996. On February 29, 2000 he received the Ph.D. degree in system science and engineering from the same university with a thesis on nonlinear control of standard and special asynchronous electric machines.

Since 1997, he has been at the Department of Electronics, Computer Science and Systems (DEIS) of the University of Bologna. On July 2000, he won a research grant from the above department on modeling and control of complex electromechanical systems. Starting from October 1, 2001, he is a Research Associate at DEIS.

His current research interests include applied nonlinear control techniques, adaptive observers, electric drives, automotive systems, power electronics equipments, active power filters and DSP-based control architectures.

View publication stats